

## The study on the ability to treat picric acid in water using the indirect photoelectrocatalytic oxidation method with a WO<sub>3</sub>/Cu electrode

Dinh Trong Nghia<sup>1\*</sup>, Le Thi Thuy Nguyen<sup>1</sup>, Ngo Tien Quyet<sup>2</sup>, Vu Thi Vui<sup>1</sup>

<sup>1</sup>Institute of New Technology, Academy of Military Science and Technology, 17 Hoang Sam, Cau Giay, Hanoi, Vietnam;

<sup>2</sup>University of Science, Vietnam National University, 334 Nguyen Trai, Thanh Xuan, Hanoi, Vietnam.

\*Corresponding author: trongnghiacnm2020@gmail.com

Received 10 Mar. 2025; Revised 26 Apr. 2025; Accepted 09 May 2025; Published 25 May 2025.

DOI: <https://doi.org/10.54939/1859-1043.j.mst.103.2025.65-73>

### ABSTRACT

*The article presents the results of a study on the fabrication and evaluation of certain properties, morphology, crystal structure of the WO<sub>3</sub> coating on a Cu substrate. Simultaneously, the article introduces the preliminary results of evaluating the ability to treat picric acid in water using the indirect electrochemical oxidation method with a WO<sub>3</sub>/Cu electrode and HOCl as the oxidizing agent. The research results show that the WO<sub>3</sub> coating on Cu substrate has a hexagonal crystal structure, a density of 6.422 g/cm<sup>3</sup>, an absorption intensity of 0.8 a.u (λ = 420 nm), and an energy bandgap of approximately 2.8 eV. With an applied potential of +0.8 V (vs. Ag/AgCl) to the WO<sub>3</sub>/Cu electrode, the indirect photoelectrochemical oxidation method using the WO<sub>3</sub>/Cu electrode and HOCl as the oxidizing agent achieves a 95% treatment efficiency for TNP at a concentration of 80 mg/L after 105 minutes at room temperature.*

**Keywords:** Tungsten trioxide; Electrochemical; TNP.

### 1. INTRODUCTION

2,4,6-Trinitrophenol (TNP), also known as picric acid, is a highly explosive organic compound widely used in the defense industry, dye production, pharmaceuticals, and pigments. Due to its high toxicity, stability, difficulty in biodegradation, and accumulation in aquatic environments, TNP has a negative impact on ecosystems and human health [1].

Recently, several solutions have been proposed for treating compounds containing the phenol ring in general and nitrophenol compounds in particular in wastewater, including oxidation [2], electrochemical [3], adsorption [4], biological degradation [5], etc. In which, indirect electrochemical oxidation (EC) is a method gaining significant attention due to its effective treatment capabilities, minimal chemical usage, and reduction of secondary waste generation [6]. This method operates based on the main mechanism of dissociating compounds to generate strong oxidizing agents such as OH<sup>•</sup>, O<sub>3</sub>, HOCl, and OCl<sup>-</sup>, which then attack and degrade organic compounds [6-7]. Despite its many advantages, the EC method still has limitations due to the occurrence of electrode corrosion. In order to overcome this limitation, several solutions have been proposed to reduce corrosion and extend the lifespan of the electrodes, such as the fabrication of inert electrodes: inert electrode fabrication (graphite, BDD, Fe<sub>5</sub>Si<sub>3</sub>, TiO<sub>2</sub>, PbO<sub>2</sub>,...), coating with conductive oxides (RuO<sub>2</sub>, IrO<sub>2</sub>,...) or applying semiconductor oxides activated by light (TiO<sub>2</sub>, ZnO, Ta<sub>2</sub>O<sub>5</sub>, BiVO<sub>4</sub>,...) [8]. Recently, WO<sub>3</sub> has attracted significant research attention due to its unique physicochemical properties such as electrochromism, photocatalysis, and photochromism. WO<sub>3</sub> is a typical n-type metal oxide with an energy bandgap ranging from 2.4 – 2.8 eV, capable of absorbing energy in the UV region and part of the visible light spectrum. Additionally, it is inexpensive, easy to synthesize, and stable in acidic and neutral environments, making WO<sub>3</sub> an ideal material for coatings in the fabrication of anodes in electrochemical systems [9].

In order to contribute further to the aforementioned research direction, focusing on the treatment of TNP contamination in wastewater from defense production, this paper presents the

results of the study on the fabrication and evaluation of several properties, morphology, chemical composition, and characteristic bonding of the  $\text{WO}_3$  coating on a Cu substrate. At the same time, it introduces the preliminary results of evaluating the ability to treat picric acid in water using the indirect photoelectrocatalytic oxidation method (PEC) with the  $\text{WO}_3/\text{Cu}$  electrode and  $\text{HOCl}$  as the oxidizing agent.

## 2. MATERIALS AND METHODS

### 2.1. Chemicals and equipment

#### 2.1.1. Chemicals

Acid picric ( $\text{C}_6\text{H}_3\text{N}_3\text{O}_7$ ) 98%, Vietnam;  $\text{Na}_2\text{WO}_4 \cdot 2\text{H}_2\text{O}$ , HCl and other chemicals (NaCl, KCl,  $\text{Na}_2\text{SO}_4$ , Etanol, Pluronic ( $\text{P}_{188}$ )): PA, S.I Analytics, China.

#### 2.1.2. Equipment

FE-SEM Hitachi S-4800, Japan; UV-Vis DRS spectroscopy, Jasco International, Japan; D8 Advance, Bruker, Germany; COD HI839800-02, Hanna Instruments, USA; HPLC1100, Agilent, USA; Vera magnetic stirrer, Cole Parmer, USA; DC power supply Agilent, E3631 DE3, USA; LED lamp, Philips, China, and other available instruments and equipment from the Institute of New Technology.

#### 2.1.3. Experimental model

The experimental model designed to evaluate the ability to treat picric acid in water using the indirect photoelectrocatalytic oxidation method with the  $\text{WO}_3/\text{Cu}$  electrode and  $\text{HOCl}$  as the oxidizing agent was referenced from the publication [10]. The general schematic of the experimental model is as follows:

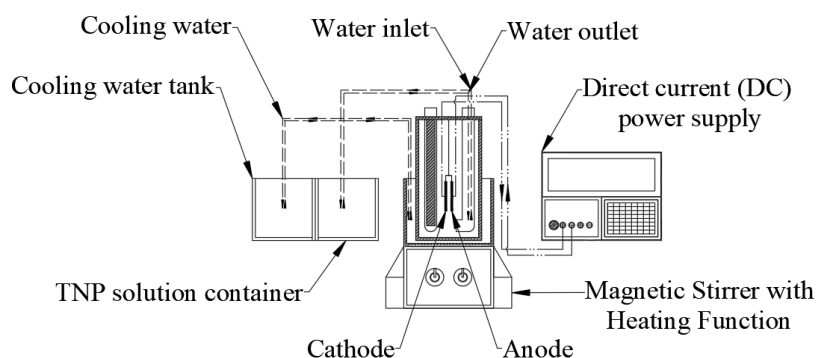


**Figure 1.** Experimental model to study and evaluate the ability to treat picric acid.

In this setup, the reaction vessel with a capacity of 1 L is made from 2 mm thick acrylic material, in the shape of a tube with a flat bottom. The vessel is equipped with two 420 nm wavelength LED lamps, each with a power of 10 W. The reaction vessel is placed inside a 5 L glass cooling bath, which is fitted with a built-in temperature sensor for measurement and display.

#### 2.1.4. Fabrication of materials

The  $\text{WO}_3$  coating is synthesized using the hydrothermal method: First, cut, clean, and smooth the surface of the Cu substrate with an area of  $24 \text{ cm}^2$  ( $80 \times 30 \times 1 \text{ mm}$ ), where the coating area is  $15 \text{ cm}^2$  ( $50 \times 30 \text{ mm}$ ). Prepare 80 mL of the coating solution consisting of 1.5 g  $\text{Na}_2\text{WO}_4 \cdot 2\text{H}_2\text{O}$ ; 0.5 g NaCl; 1 g  $\text{P}_{188}$ , and 80 mL of distilled water. Adjust the pH of the solution to 2 - 3 using 1M HCl. Transfer the solution into a 100 mL Teflon flask, then place the Cu substrate into the Teflon container, seal the lid tightly, and carry out the reaction at  $180 \text{ }^\circ\text{C}$  for 4 - 12 hours continuously. After the reaction is completed, remove the Cu substrate and rinse it gently with distilled water until the surface has a neutral pH (tested using litmus paper). Dry it at  $80 \text{ }^\circ\text{C}$  for 10 hours, then at

120 °C for another 10 hours, and finally calcine it at 300 °C for 2 hours. Allow the sample to cool naturally, then collect the sample for further analysis.

## **2.2. Research methods**

*2.2.1. Research on evaluating some properties, morphology, crystal structure, radiation absorption capacity of WO<sub>3</sub> coating on Cu substrate*

### **a. Study on surface morphology**

The surface morphology of the WO<sub>3</sub>/Cu photoanode coating was analyzed using the FE-SEM Hitachi S-4800 device at the Institute of Materials Science/Institute of Science and Technology, Vietnam Academy of Science and Technology.

### **b. Determining the crystal structure and radiation absorption capability of the WO<sub>3</sub> coating**

The crystal structure of WO<sub>3</sub> was determined through X-ray diffraction (XRD) using the D8 Advance device, Bruker, Germany, at the Institute of Chemistry/Institute of Science and Technology, Vietnam Academy of Science and Technology. The radiation absorption capability was measured using the UV-Vis-DRS spectroscopy method with the V-770 device Jasco International, Japan, at the Institute of Materials Science/Institute of Science and Technology, Vietnam Academy of Science and Technology.

*2.2.2. Study on the ability to treat picric acid in water using the PEC method with a WO<sub>3</sub>/Cu electrode and HOCl as the oxidizing agent*

### **a. Comparison of the TNP treatment efficiency of PEC, EC, and PC**

The experiment comparing the TNP treatment efficiency of the PEC, EC, and PC solutions using the WO<sub>3</sub>/Cu electrode was conducted under the following conditions: V = 0.8 V (vs. Ag/AgCl), S<sub>WO<sub>3</sub>/Cu</sub> = 15 cm<sup>2</sup>, pH = 3 - 4, C<sub>NaCl</sub> = 0.15 M, W = 10 W, λ = 420 nm, C<sub>TNP</sub> = 50 mg/L, and a reaction time of 120 minutes. The TNP treatment efficiency was determined using the following formula:

$$H\% = \frac{C_0 - C_t}{C_0} \times 100 (\%) \quad (1)$$

Including H is the treatment efficiency (%), C<sub>0</sub> and C<sub>t</sub> are the TNP concentrations at the initial time and time t, respectively (mg/L).

### **b. Evaluation of the effect of C<sub>NaCl</sub>**

The experiment investigating the effect of C<sub>NaCl</sub> on the TNP treatment efficiency using the PEC method with the WO<sub>3</sub>/Cu electrode was conducted under the following conditions: V = 0,8 V (vs. Ag/AgCl), S<sub>WO<sub>3</sub>/Cu</sub> = 15 cm<sup>2</sup>, pH = 3 - 4, W = 10 W, λ = 420 nm, C<sub>TNP</sub> = 50 mg/L, reaction time of 150 minutes, with C<sub>NaCl</sub> ranging from 0.05 M to 0.2 M. The TNP treatment efficiency was determined using the following formula (1).

### **c. Evaluation of the effect of initial C<sub>TNP</sub>**

The experiment investigates the influence of the initial TNP concentration on the TNP removal efficiency using the PEC method with the WO<sub>3</sub>/Cu electrode, conducted under the following conditions: V = 0.8 V (vs. Ag/AgCl), pH = 3 - 4, C<sub>NaCl</sub> = 0.15M, W = 10 W, λ = 420 nm, time = 105 min, and initial TNP concentrations of 20 mg/L; 40 mg/L; 60 mg/L; 80 mg/L; 100 mg/L; 120 mg/L; 140 mg/L. The TNP removal efficiency is determined according to formula (1).

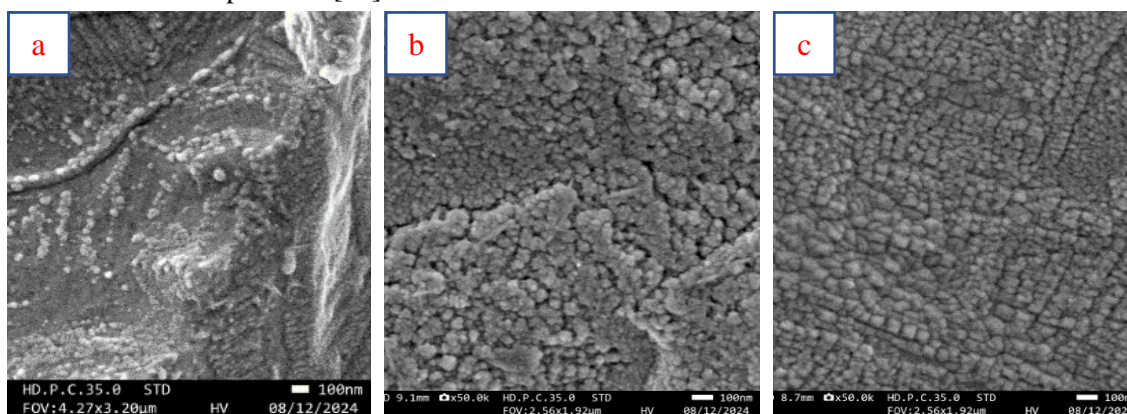
## **3. RESULTS AND DISCUSSION**

### **3.1. Results of evaluating the properties, morphology, chemical composition, and characteristic bonding of the WO<sub>3</sub> coating on Cu substrate**

#### *a. Regarding the morphology*

The FE-SEM analysis results of the WO<sub>3</sub> coating synthesized by the direct hydrothermal

method on a Cu substrate at pH 2 - 3, using  $\text{Na}_2\text{WO}_4$  and  $\text{P}_{188}$  for reaction times of 4, 8, and 12 hours (figure 2), show results that are quite consistent with previous reports. Specifically, after 4 hours of hydrothermal treatment, connections between the  $\text{WO}_3$  material and CuO appear. After 8 hours, the  $\text{WO}_3$  particles form a uniform coating on the Cu substrate, and after 12 hours, the particles are distributed quite densely with relatively uniform sizes. The process of forming the  $\text{WO}_3$  coating occurs in three stages: bond formation, anisotropic crystallization, and the formation of nanometer-sized particles [11].



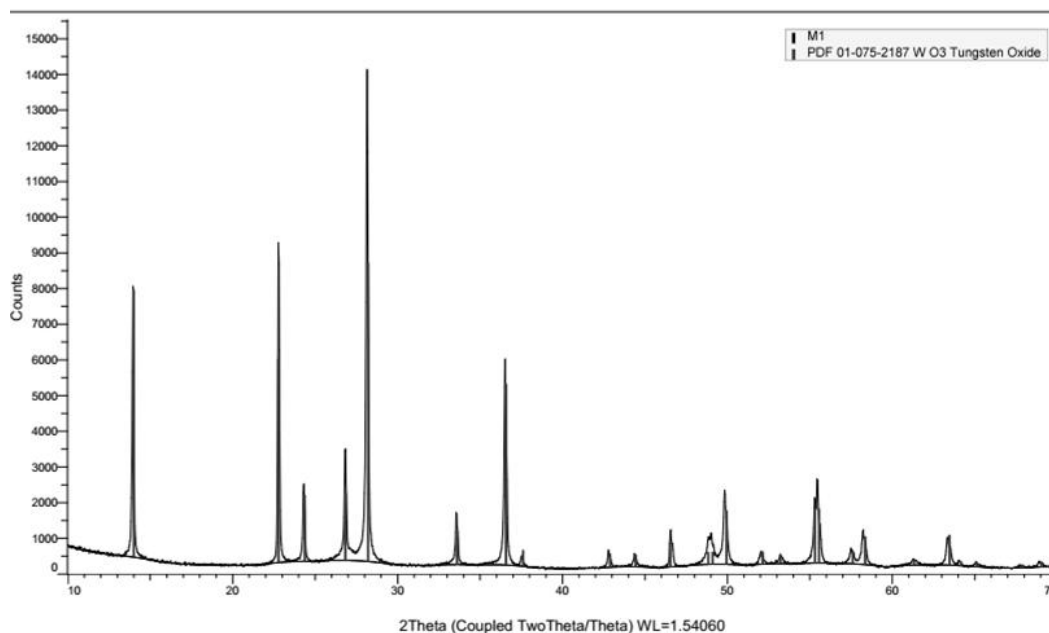
**Figure 2.** FE-SEM images of  $\text{WO}_3/\text{Cu}$ .

Figure 2 (a, b, c): Images of the  $\text{WO}_3/\text{Cu}$  anode after 4, 8, and 12 hours of hydrothermal treatment.

The formation of the  $\text{WO}_3$  coating helps create a double layer of charge due to the ion separation on the electrode surface, and the electrostatic forces between them will slow down the diffusion of  $\text{Cu}^{2+}$  during electrolysis, thereby increasing the lifespan of the electrode [12].

*b. Regarding the chemical composition and characteristic bonding of the  $\text{WO}_3$  coating*

The results of the chemical composition analysis of the  $\text{WO}_3$  coating on the Cu substrate, determined by X-ray diffraction (XRD), are presented in figure 3.



**Figure 3.** X-ray diffraction (XRD) pattern of the  $\text{WO}_3$  coating.

The X-ray diffraction (XRD) pattern of the WO<sub>3</sub> coating in figure 3 shows three sharp diffraction peaks with strong intensity at 2θ angles of 14.1°; 22.9°; 28.2° corresponding to the crystal planes (010), (001), (200), respectively. Additionally, there are lower-intensity diffraction peaks at 2θ angles of 36.8°; 49.5°; 58.8° corresponding to the crystal planes (110), (011), (002), characteristic of the hexagonal, monoclinic WO<sub>3</sub> phase, belonging to the P6/mmm (191) space group (according to the JCPDS card: 01-075-2187). For the hexagonal crystal phase in the P6/mmm space group, the atoms are arranged symmetrically around a main axis, characterized by high symmetry.

The radiation absorption capability of the WO<sub>3</sub> coating after fabrication was evaluated using the UV-Vis-DRS spectroscopy method, with a scanning wavelength range from 200 nm to 1400 nm, a scan speed of 400 nm/min, and a D2/WI light source. The analysis results are presented in figure 4.

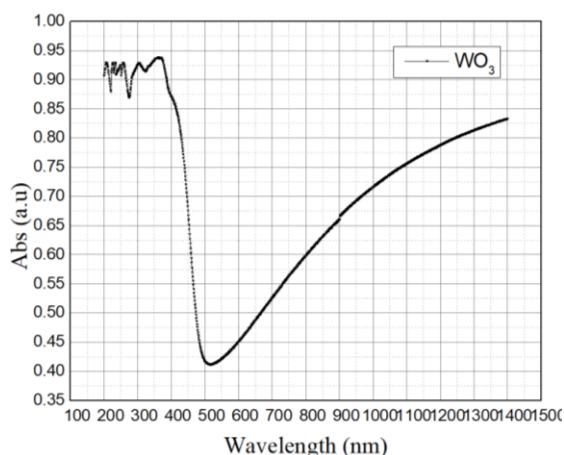


Figure 4. UV-Vis-DRS spectrum of the WO<sub>3</sub> coating.

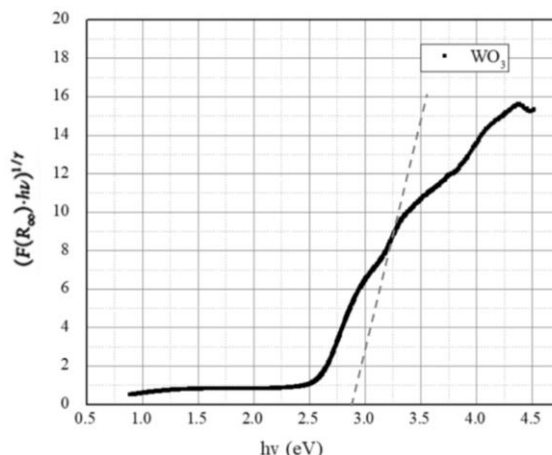


Figure 5. Energy bandgap  $E_g$  of the WO<sub>3</sub> coating.

The results show that at shorter wavelengths (200 - 420 nm), strong absorption peaks appear due to significant electronic transitions, with an absorption intensity reaching around  $\pm 0.9$  a.u. This indicates that the WO<sub>3</sub> material, after fabrication, has strong absorption capability in the ultraviolet region and partially in the visible region.

Meanwhile, using the Kubelka-Munk function calculated according to formula (2), by extrapolating the linear segment in the graph of  $(F(R_\infty) \cdot hv)^{1/\gamma}$  versus  $h\nu$  corresponding to approximately 2.8 eV, the energy bandgap value  $E_g$  of the WO<sub>3</sub> coating can be determined (figure 5) [13].

$$(F(R_\infty) \cdot hv)^{1/\gamma} = B(h\nu - E_g) \quad (2)$$

Thus, from the results displayed in the absorption spectrum and the determination of  $E_g$  using the Kubelka-Munk function, it can be further confirmed that the WO<sub>3</sub> coating has good absorption of ultraviolet light and part of the visible light spectrum. Therefore, using the procedure outlined in section 2.1.3, a successful WO<sub>3</sub> coating was fabricated on a Cu substrate, with morphological characteristics and properties similar to those reported in previous studies [12-13].

### 3.2. Results of the study on the ability to treat picric acid in water using the PEC method with WO<sub>3</sub>/Cu electrode and HOCl as the reactive agent

#### a. Comparison of the TNP treatment efficiency of PEC, EC, and PC

The survey results show that the PEC solution has the best efficiency in treating TNP, followed by the PC solution with lower treatment efficiency, while the EC solution is ineffective in treating TNP (figure 6). This result proves that the PEC solution can generate free chlorine species (FCS),

while EC cannot generate FCS under the applied potential of + 0,8 V (vs. Ag/AgCl), which is lower than the minimum potential of 1,36 V (vs. NHE) required for chloride ion oxidation. PC, having no applied potential, cannot generate FCS.

According to Koo et al (2019) [9], under the influence of visible light, the holes ( $h^+$ ) generated by the  $WO_3$  coating will oxidize  $Cl^-$  ions and form dissolved  $Cl_2(aq)$ . The  $Cl_2$  gas then undergoes hydrolysis and reacts with water to produce HOCl and HCl. This process occurs vigorously in acidic environments with a pH range from 3 to 5 (equations 3 and 4). These are the necessary conditions for the PEC solution to operate effectively.



*b. Investigation of the effect of NaCl concentration*

The results of the investigation into the effect of NaCl concentration on TNP treatment efficiency are shown in figure 7, indicating that the current density increases as  $C_{NaCl}$  increases. However, the current density decreases over time due to the consumption of  $Cl^-$  ions near the anode surface [16].

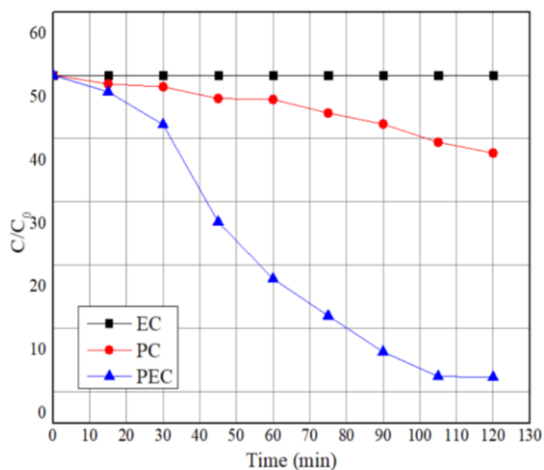


**Figure 6.** TNP treatment efficiency of PEC, PC and EC.

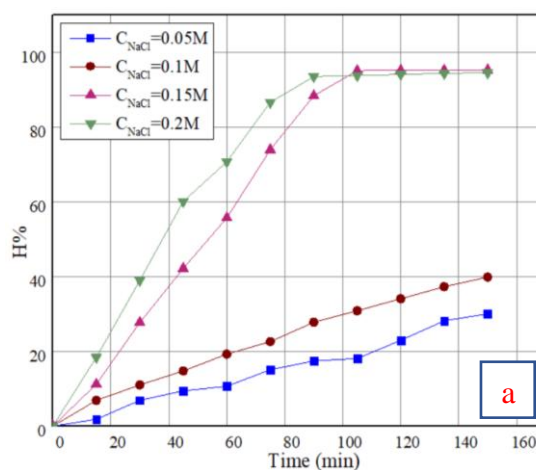


**Figure 7a.** Effect of  $C_{NaCl}$  on the TNP treatment process.

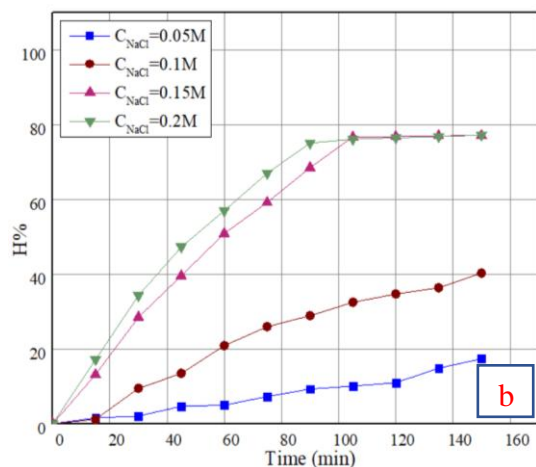


**Figure 7b.** Effect of  $C_{NaCl}$  on the COD treatment process.

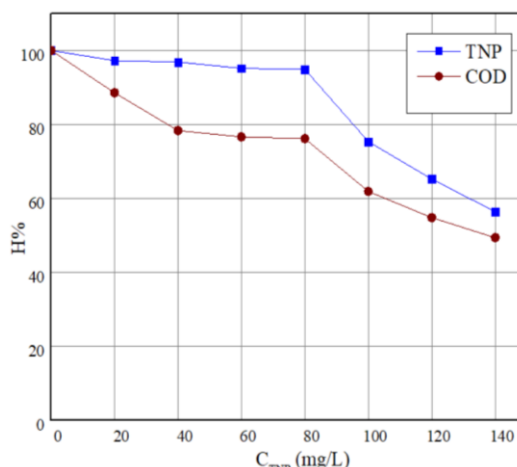


**Figure 8.** Effect of initial  $C_{TNP}$  on the TNP, COD treatment process.

As the NaCl concentration increases in the range of 0.05 M; 0.1 M; 0.15 M; and 0.2 M; the TNP treatment efficiency also increases, reaching 30%; 39.9%; 94.5%; and 95.2% respectively (figure 7a), meanwhile the COD value of the treated solution is reduced to 17.4%; 40.3%; 77.2%; 77.1% after 150 minutes of treatment (figure 7b). However, when the NaCl concentration increases from 0.15 M to 0.2 M, and after 105 minutes of treatment, both the TNP treatment efficiency and COD remain almost unchanged. This could be due to the saturation of HOCl in the solution at high NaCl concentrations, where the excess HOCl increases but does not improve the treatment efficiency, as the reaction rate has reached the dynamic equilibrium limit [9]. Thus, a NaCl concentration of 0.15 M and a treatment time of 105 minutes are the optimal conditions for effective TNP treatment in water under the experimental conditions mentioned above.

*c. Effect initial TNP concentration*

The research results show that the treatment efficiency of TNP tends to decrease as the initial TNP concentration increases. Specifically, when  $C_{TNP}$  increases from 20 mg/L to 140 mg/L, the treatment efficiency drops from 93.4% to 56.6% (figure 8). For  $C_{TNP} \geq 80$  mg/L, the TNP and COD treatment efficiencies show a significant decrease, which could be due to the insufficient amount of HOCl in the PEC to oxidize TNP. Additionally, according to Liang et al [17] the intermediate products of the TNP oxidation process may continue to be oxidized, slowing down the reaction and reducing the treatment efficiency.

Thus, the optimal conditions for the PEC solution to treat TNP in water are as follows: initial  $C_{TNP} \leq 80$  mg/L, pH = 3 - 4,  $C_{NaCl} = 0.15$  M, and a treatment time of 105 minutes.

*d. The mechanism for TNP treatment*

Under the influence of visible light, the  $WO_3$  coating can oxidize  $Cl^-$  ions without requiring a potential  $\geq 1.36$  V (vs. NHE) [16]. This mechanism not only helps reduce energy consumption but also decreases the risk of HOCl being oxidized into  $ClO^\bullet$  or  $OCl^-$  with a potential  $\geq 1.48$  V (vs. NHE), thus minimizing the formation of harmful by-products such as trihalomethanes, chloramines, chlorinated phenols,... [10]. On the other hand, the molecular structure of TNP consists of three  $NO_2^-$  groups at positions 2, 4, and 6, and a hydroxyl group ( $OH^-$ ) at position 1. The aromatic ring exhibits strong electron-donating properties at the ortho and meta positions. The treatment of TNP with HOCl mainly occurs through an electron substitution reaction on the aromatic ring. At pH values from 3 - 4, HOCl is an effective oxidizing agent, and it tends to attack the un-substituted positions, forming intermediate products (CABs) [18]. The oxidation mechanism of TNP in PEC may proceed as follows:

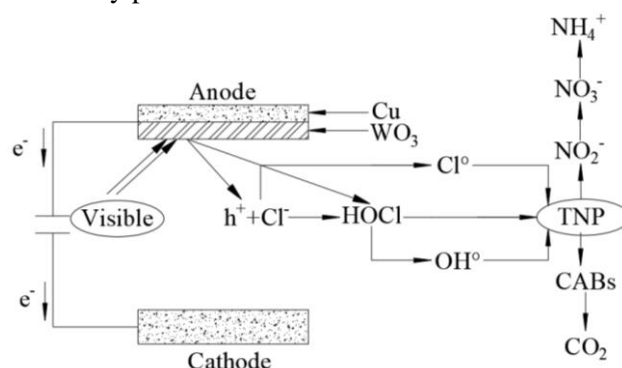


**Figure 9.** Oxidation mechanism of TNP by the PEC method.

**4. CONCLUSIONS**

The research team successfully synthesized a  $WO_3$  coating on a Cu substrate using the hydrothermal method, applied in the PEC method to treat TNP contamination in water. The  $WO_3$

coating after fabrication has a hexagonal crystal structure, an energy bandgap of approximately 2.8 eV, and the ability to absorb light in the UV region and part of the visible light spectrum, operating stably in low pH environments. The PEC solution effectively treats TNP with an initial concentration of 80 mg/L, achieving a treatment efficiency of 95% after 105 - 120 minutes through the mechanism of HOCl generation by oxidizing  $\text{Cl}^-$  ions with the  $\text{WO}_3/\text{Cu}$  anode at a potential of +0.8 V (vs.  $\text{Ag}/\text{AgCl}$ ), helping to reduce energy consumption and avoid the formation of chlorine by-products. Factors such as NaCl concentration, treatment time, and initial TNP concentration significantly affect the treatment efficiency.

## REFERENCES

- [1]. "Picric-Acid @ pubchem.ncbi.nlm.nih.gov." [Online]. Available: <https://pubchem.ncbi.nlm.nih.gov/compound/Picric-Acid>
- [2]. J. Gong, Y. Liu, and X. Sun, " $\text{O}_3$  and UV/ $\text{O}_3$  oxidation of organic constituents of biotreated municipal wastewater," *Water Res.*, vol. 42, no. 4, pp. 1238–1244, (2008), doi: <https://doi.org/10.1016/j.watres.2007.09.020>.
- [3]. E. Brillas, I. Sirés, and M. A. Oturan, "*Electro-Fenton process and related electrochemical technologies based on Fenton's reaction chemistry*," *Chem. Rev.*, vol. 109, no. 12, pp. 6570–6631, (2009), doi: [10.1021/cr900136g](https://doi.org/10.1021/cr900136g).
- [4]. D. Tang, Z. Zheng, K. Lin, J. Luan, and J. Zhang, "*Adsorption of p-nitrophenol from aqueous solutions onto activated carbon fiber*," *J. Hazard. Mater.*, vol. 143, no. 1, pp. 49–56, (2007), doi: <https://doi.org/10.1016/j.jhazmat.2006.08.066>.
- [5]. R. M. Farsi et al., "*Biodegradation of picric acid (2,4,6-trinitrophenol, TNP) by free and immobilized marine Enterococcus thailandicus isolated from the red sea, Saudi Arabia*," *Egypt. J. Aquat. Res.*, vol. 47, no. 3, pp. 307–312, (2021), doi: <https://doi.org/10.1016/j.ejar.2021.05.002>.
- [6]. C. A. Martínez-Huitle and S. Ferro, "*Electrochemical oxidation of organic pollutants for the wastewater treatment: direct and indirect processes.*," *Chem. Soc. Rev.*, vol. 35, no. 12, pp. 1324–1340, (2006), doi: [10.1039/b517632h](https://doi.org/10.1039/b517632h).
- [7]. S. Wang, D. Zhong, G. Qu, P. Ning, J. Quan, and X. Chen, "*Degradation of phenol in wastewater with ozone produced by self-design ozone generator*," vol. 02002, (2016).
- [8]. W. S. Koo, J. W. Lee, W. C. Chong, Y. L. Pang, and L. C. Sim, "*An overview of photocatalytic degradation: photocatalysts, mechanisms, and development of photocatalytic membrane*," *Environ. Sci. Pollut. Res.*, vol. 27, no. 3, pp. 2522–2565, (2020), doi: [10.1007/s11356-019-07193-5](https://doi.org/10.1007/s11356-019-07193-5).
- [9]. M. S. Koo, X. Chen, K. Cho, T. An, and W. Choi, "*In Situ photoelectrochemical chloride activation using a  $\text{WO}_3$  electrode for oxidative treatment with simultaneous  $\text{H}_2$  evolution under visible light*," *Environ. Sci. Technol.*, vol. 53, no. 16, pp. 9926–9936, (2019), doi: [10.1021/acs.est.9b02401](https://doi.org/10.1021/acs.est.9b02401).
- [10]. Y. Wang, Y. Xue, and C. Zhang, "*Generation and application of reactive chlorine species by electrochemical process combined with UV irradiation: Synergistic mechanism for enhanced degradation performance*," *Sci. Total Environ.*, vol. 712, p. 136501, (2020), doi: <https://doi.org/10.1016/j.scitotenv.2020.136501>.
- [11]. F. Zheng et al., "*Tertiary structure of cactus-like  $\text{WO}_3$  spheres self-assembled on Cu foil for supercapacitive electrode materials*," *Journal of Alloys and Compounds*, vol. 712, pp. 345–354, (2017). doi: [10.1016/j.jallcom.2017.04.094](https://doi.org/10.1016/j.jallcom.2017.04.094).
- [12]. L. Knijff, M. Jia, and C. Zhang, "*Electric double layer at the metal-oxide/electrolyte interface*," K. Wandelt and G. B. T.-E. of S.-L. I. (First E. Bussetti, Eds., Oxford: Elsevier, pp. 567–575, (2024). doi: <https://doi.org/10.1016/B978-0-323-85669-0.00012-X>.
- [13]. P. Makuła, M. Pacia, and W. Macyk, "*How to correctly determine the band gap energy of modified semiconductor photocatalysts based on UV-Vis spectra*," *J. Phys. Chem. Lett.*, vol. 9, no. 23, pp. 6814–6817, (2018), doi: [10.1021/acs.jpcclett.8b02892](https://doi.org/10.1021/acs.jpcclett.8b02892).
- [14]. D. Sánchez-Martínez and D. B. Hernandez-Uresti, "*Chapter 13 - Nanostructured-based  $\text{WO}_3$  photocatalysts: Recent development, activity enhancement, perspectives and applications for wastewater treatment*," E. I. García-López and L. B. T.-M. S. in P. Palmisano, Eds., Elsevier, pp. 211–220, (2021). doi: <https://doi.org/10.1016/B978-0-12-821859-4.00008-8>.

- [15].P. Kolhe, P. Shirke, N. Maiti, M. More, and K. Sonawane, "Facile hydrothermal synthesis of  $WO_3$  nanoconifer thin film: Multifunctional behavior for gas sensing and field emission applications," J. Inorg. Organomet. Polym. Mater., vol. 29, (2019), doi: 10.1007/s10904-018-0962-0.
- [16].Z. Tasic, V. K. Gupta, and M. M. Antonijevic, "The mechanism and kinetics of degradation of phenolics in wastewaters using electrochemical oxidation," Int. J. Electrochem. Sci., vol. 9, no. 7, pp. 3473–3490, (2014), doi: 10.1016/s1452-3981(23)08025-2.
- [17].H. Liang, "Development of titania nanotube films for degradation of the recalcitrant organic pollutants in water", (2009).
- [18].N. Bensalah and A. Gadri, "Electrochemical oxidation of 2,4,6-Trinitrophenol on Boron-doped diamond anodes," J. Electrochem. Soc., vol. 152, pp. D113–D116, (2005), doi: 10.1149/1.1904942.

### TÓM TẮT

#### **Nghiên cứu khả năng xử lý axit picric trong nước bằng phương pháp quang oxi hóa điện hóa gián tiếp sử dụng điện cực $WO_3/Cu$**

Bài báo giới thiệu kết quả nghiên cứu chế tạo, đánh giá một số tính chất, hình thái học, cấu tạo tinh thể của lớp phủ  $WO_3$  trên nền Cu. Đồng thời, giới thiệu kết quả đánh giá bước đầu về khả năng xử lý acid picric trong nước của phương pháp oxi hóa điện hóa gián tiếp sử dụng điện cực  $WO_3/Cu$  và tác nhân  $HOCl$ . Kết quả nghiên cứu cho thấy lớp phủ  $WO_3$  trên nền Cu có cấu trúc tinh thể lục giác, khối lượng riêng  $6,422\text{ g/cm}^3$ , cường độ hấp phụ  $0,8\text{ a.u}$  ( $\lambda = 420\text{ nm}$ ), dải cấm năng lượng khoảng  $2,8\text{ eV}$ . Với điện thế áp dụng cho điện cực  $WO_3/Cu$  là  $+0,8\text{ V}$  (vs.  $Ag/AgCl$ ), phương pháp quang oxi hóa điện hóa gián tiếp sử dụng điện cực  $WO_3/Cu$  và tác nhân  $HOCl$  cho hiệu suất xử lý TNP nồng độ  $80\text{ mg/L}$  đạt  $95\%$  sau  $105\text{ phút}$  ở nhiệt độ phòng.

**Từ khóa:** Tungsten trioxide; Điện hóa gián tiếp; Acid picric; Xử lý.